

Neuroprotective effects of kojic acid and nano-kojic acid in experimental brain ischemia induced by bilateral common carotid artery occlusion

Mohammad Shokati Sayyad ¹, Majid Saeedi ^{2, 3}, Fatemeh Shaki ^{1, 2}, Fereshteh Talebpour Amiri ⁴, Reza Negarandeh ^{3, 5}, Mohammad Seyedabadi ^{1, 2*}

- ¹ Department of Toxicology and Pharmacology, Faculty of Pharmacy, Mazandaran University of Medical Sciences, Sari, Iran
- ² Pharmaceutical Sciences Research Center, Institute of Herbal Medicines and Metabolic Disorders, Mazandaran University of Medical Sciences, Sari, Iran
- ³ Department of Pharmaceutics, Faculty of Pharmacy, Mazandaran University of Medical Sciences, Sari, Iran
- ⁴ Department of Anatomy, Faculty of Medicine, Mazandaran University of Medical Sciences, Sari, Iran
- ⁵ Cellular and Molecular Biology Research Center, Health Research Institute, Babol University of Medical Sciences, Babol, Iran

ARTICLE INFO

Article type: Original

Article history: Received: Jul 22, 2025

Accepted: Sep 20, 2025 **Keywords:**Anti-oxidants

Ischemia Neuroprotection Oxidative stress

Inflammation

ARSTRACT

Objective(s): Brain ischemia remains a leading cause of death and neurological disability worldwide, with current treatments limited by narrow therapeutic windows and insufficient neuroprotection. Kojic acid (KA), a natural compound with demonstrated anti-oxidant and anti-inflammatory properties, has not been thoroughly evaluated in cerebral ischemia. Its limited brain bioavailability may have hindered the identification of its potential therapeutic effects. This study aimed to investigate the effects of both KA and its nanostructured lipid carriers (nKA) in a rat bilateral common carotid artery occlusion (BCCAO) model.

Materials and Methods: Adult male rats were randomly allocated to seven groups: sham, BCCAO, KA (1 and 10 mg/kg), nKA (1 and 10 mg/kg), and vehicle. Following BCCAO surgery, animals received intraperitoneal treatments for seven days. Behavioral assessments included the modified neurological severity score and grid walk test. Brain and serum samples were collected to evaluate histopathology, gene expression, oxidative stress markers, inflammatory cytokines, and pharmacokinetic parameters. Results: Histological analysis indicated reduced neuronal loss in both KA and nKA-treated groups. Notably, only nKA significantly improved behavioral outcomes. Both treatments reduced the proapoptotic gene BAX and the pro-inflammatory cytokine TNF-α, while nKA additionally increased Nrf2 and reduced IL-6 expression. Both formulations mitigated oxidative stress by decreasing reactive oxygen species, protein carbonylation, and malondialdehyde levels, while also increasing glutathione concentrations.

Conclusion: Nano-kojic acid showed better neurobehavioral improvements, while both forms reduced oxidative stress and inflammation, indicating neuroprotective potential. Further studies are needed to clarify mechanisms and long-term safety.

► Please cite this article as:

Shokati Sayyad M, Saeedi M, Shaki F, Talebpour Amiri F, Negarandeh R, Seyedabadi M. Neuroprotective effects of kojic acid and nano-kojic acid in experimental brain ischemia induced by bilateral common carotid artery occlusion. Iran J Basic Med Sci 2026; 29: 43-54. doi: https://dx.doi.org/10.22038/ijbms.2025.89790.19367

Introduction

Stroke, defined as a sudden interruption or significant reduction of blood and oxygen supply to a localized region of the brain, remains a leading cause of mortality and long-term disability worldwide (1). It is broadly categorized into ischemic and hemorrhagic subtypes, with ischemic stroke accounting for the majority of cases and associated with higher mortality rates (2). One of the primary contributors to ischemia is occlusion of the carotid arteries, whether unilateral or bilateral, which results in neuronal loss and disruption of normal brain functions (3). Clinically, these events present as deficits in motor coordination and cognition, and in severe cases, can be fatal. Without adequate preventive measures and therapeutic interventions,

projections estimate that ischemic stroke-related mortality could reach approximately 7.8 million deaths globally by 2030 (4, 5).

The pathophysiology of ischemic stroke is highly complex, involving a cascade of biochemical and cellular events. The initial deprivation of glucose and oxygen leads to energy failure, impaired ATP synthesis, and ionic imbalance, which in turn induces excitotoxicity, mitochondrial dysfunction, and ultimately, cell death (6, 7). A hallmark of this process is the overproduction of reactive oxygen species (ROS) and reactive nitrogen species (RNS), such as superoxide, hydrogen peroxide, and nitric oxide, which drive oxidative stress and disrupt the delicate oxidant-anti-oxidant balance in neural tissue. This imbalance results in lipid peroxidation, protein oxidation, DNA damage, and further mitochondrial

*Corresponding author: Mohammad Seyedabadi. Department of Toxicology and Pharmacology, School of Pharmacy, Mazandaran University of Medical Sciences, Sari, Iran. Email: seyedabadi1981@gmail.com, m.seyedabadi@mazums.ac.ir





impairment (8, 9), as reflected by elevated biomarkers including malondialdehyde (MDA) and protein carbonyls (PC), and depletion of endogenous anti-oxidants like glutathione (GSH). The Nrf2/HO-1 signaling pathway is a critical endogenous defense mechanism, regulating the expression of cytoprotective genes and playing a key neuroprotective role during ischemia-reperfusion injury (9-11).

Concomitantly, neuroinflammation is initiated by damage, releasing pro-inflammatory cytokines such as tumor necrosis factor-alpha (TNF- α) and interleukin-6 (IL-6). This inflammatory cascade promotes blood-brain barrier (BBB) disruption and further neuronal damage (12, 13). Additional markers such as lactate dehydrogenase (LDH) and nitric oxide further indicate ongoing tissue injury and inflammation. The interplay between proapoptotic (BAX) and anti-apoptotic (BCL2) proteins also critically determines neuronal survival following ischemic insult (14-16).

Under physiological conditions, the brain relies on a network of anti-oxidant defense systems, including both enzymatic and non-enzymatic mechanisms, that counteract the damaging effects of ROS and maintain redox homeostasis. However, when these protective systems are overwhelmed or impaired, oxidative damage accumulates, leading to neuronal dysfunction and increased vulnerability to neurodegeneration (17, 18).

The bilateral common carotid artery occlusion (BCCAO) model is widely used in rodents to mimic human cerebral ischemia or ischemic stroke, providing a reproducible and clinically relevant platform for investigating the mechanisms of ischemic injury and evaluating potential therapeutic interventions. While current pharmacological strategies for ischemic stroke focus primarily on restoring blood flow, there is a growing recognition of the need for adjunctive therapies that target the secondary injury cascades of oxidative stress and inflammation, which are not adequately addressed by reperfusion alone (19, 20). So, two primary pharmacological strategies are employed in ischemic stroke: reopening blocked blood vessels and protecting against ischemia-reperfusion injury. The latter is particularly important as it involves inflammatory cascades and oxidative stress triggered by various gene and molecular factors, upon reoxygenation of the ischemic cells, leading to tissue damage (21).

Kojic acid (KA), a natural secondary metabolite first isolated from Aspergillus oryzae, has gained considerable attention for its potent anti-oxidant and anti-inflammatory properties. As a metal chelator, KA inhibits ROS generation and lipid peroxidation, thereby mitigating oxidative stress (22, 23). Preclinical studies have demonstrated that KA can reduce oxidative stress markers, enhance the expression of Nrf2 and HO-1, and suppress neuroinflammatory pathways, including the inhibition of TNF-a and IL-1β production. These effects have been observed in models of neuroinflammation and neurodegeneration, where KA administration led to reductions in ROS and lipid peroxidation, an increase in cytoprotective genes, and improved functional outcomes. These mechanistic insights provide a compelling rationale for evaluating KA as a neuroprotective agent in ischemic stroke, where both oxidative and inflammatory cascades are central to neuronal injury (24, 25). These findings provide a strong mechanistic rationale for evaluating KA in the context of cerebral ischemia, where both oxidative and inflammatory cascades are prominent contributors to neuronal injury.

Despite these promising preclinical findings, the

therapeutic application of KA in cerebral ischemia has been limited by its poor bioavailability and restricted brain penetration. Nanoparticle-based drug delivery systems, such as nano-kojic acid (nKA) formulations, have been developed to overcome these challenges by enhancing pharmacokinetic properties, tissue distribution, and targeted delivery (26-28). Encapsulation within nanoparticles can improve the stability and solubility of KA, potentially amplifying its beneficial effects on oxidative stress and inflammation in the context of cerebral ischemia.

By these considerations, the present study aims to investigate the neuroprotective effects of KA and its nanoformulation in a rat model of cerebral ischemia induced by BCCAO. We employ a comprehensive approach, including biochemical and histological analyses, evaluation of key gene pathways, assessment of behavioral changes related to inflammation and oxidative stress, and quantification of drug levels in the brain using high-performance liquid chromatography (HPLC).

Materials and Methods

Chemicals

KA was obtained from Sigma Aldrich (United Kingdom, USA). Acetonitrile and ketamine were sourced from Merck (Germany), and xylazine was purchased from Alfasan (Woerden, Netherlands). All other chemicals used in this study were of analytical grade and utilized without further purification.

Animals

Fifty-six male Wistar rats, weighing 200–220 g and aged 12–13 weeks, were obtained from the Animal Laboratory of Mazandaran University of Medical Sciences (Sari, Iran). Animals were housed under standard laboratory conditions with ad libitum access to food and water. All experimental procedures were approved by the Committee of Animal Experimentation at Mazandaran University of Medical Sciences and conducted in accordance with the National Institutes of Health Guide for the Care and Use of Laboratory Animals (IR.MAZUMS.AEC.1403.018).

Experimental design and animal groups

The rats were randomly assigned to seven groups, with eight animals in each group, as outlined in Table 1. Brain ischemia was induced using a standardized protocol, and animals received daily intraperitoneal injections of KA, nKA acid, or vehicle. On the seventh day following brain ischemia induction, behavioral assessments, including the Grid Walk test and the Modified Neurological Severity Score (mNSS), were performed to evaluate motor coordination and neurological function. On the eighth day, rats were deeply anesthetized and sacrificed in the Institute for Experimental Animal Research of our university. After confirming the absence of reflexes for deep pain, the animals were beheaded, the skull was immediately opened, and

Table 1. Animal groups (8 rats in each group)

| Description |
|-------------------------------------|
| Control (without ischemia and drug) |
| Brain ischemia (without drug) |
| Brain ischemia + KA 1 mg/kg |
| Brain ischemia + KA 10 mg/kg |
| Brain ischemia + nKA 1 mg/kg |
| Brain ischemia + nKA 10 mg/kg |
| Brain ischemia + vehicle |
| |



brain tissues were collected for analyses of oxidative stress markers, gene expression, and HPLC quantification. At the same time, serum samples were prepared for subsequent biochemical evaluations. The samples were stored as mentioned in each section.

Induction of brain ischemia (cerebral ischemia/reperfusion)

Brain ischemia was induced in rats using the BCCAO technique, as previously validated in preclinical studies. Animals were anesthetized by intraperitoneal injection of ketamine (75 mg/kg) and xylazine (10 mg/kg). A midline cervical incision (~1 cm) was made to expose both common carotid arteries, identified by their distinct pulsatile morphology. The arteries were isolated from adjacent vagal tissue and bilaterally occluded with microvascular clamps for 20 min to induce transient global ischemia. Subsequent clamp removal restored cerebral reperfusion, after which the surgical site was closed with sutures. Postoperative treatments were administered intraperitoneally for seven consecutive days, with tissue and serum samples collected immediately after behavioral tests. Sham-operated controls underwent identical surgical exposure without arterial occlusion, ensuring procedural equivalence while maintaining baseline cerebral perfusion (3, 29).

Synthesis of nano-kojic acid

The nanostructured lipid carriers (NLCs) containing KA are fabricated based on a melt emulsification followed by the ultrasonication technique. Briefly, the lipid phase consisting of cholesterol, oleic acid, glyceryl monostearate (GMS), and Span 60 was heated to 90-95 °C until fully melted, then mixed evenly. In a separate beaker, the aqueous phase, which contains deionized water and Tween 20, was mixed and then heated to the same temperature as the oily phase. Subsequently, two-thirds of the aqueous phase with KA is added dropwise to the lipid phase under high-speed stirring to form a pre-emulsion. The mixture then undergoes 5 min of 100% amplitude probe sonication (Bandelin, 3100, Germany). After the first sonication period, the remaining one-third of the water phase in an ice-water bath was added to the mixture, which was then quickly placed in the bath. Finally, the mixture was sonicated for 5 min and allowed to cool at room temperature (30).

Small-animal PET imaging (Micro PET)

Cerebral glucose metabolism was assessed using a small-animal PET scanner (Xtrim PET) at the Preclinical Core Facility (TPCF) of Tehran University of Medical Sciences, Iran. Before imaging, rats underwent an 8-hour fasting period with ad libitum water access. Under general anesthesia (ketamine/xylazine), animals received a tail vein injection of 18F-fluorodeoxyglucose (18F-FDG; 0.7 mCi) and were allowed a 60-minute awake uptake period to minimize anesthesia-related metabolic interference. Imaging was performed in the prone position using a dedicated rodent bed, with raw data reconstructed into coronal, sagittal, and axial planes (31, 32).

Behavioral tests

To evaluate behavioral and motor impairments seven days after BCCAO-induced brain ischemia, two established tests were employed: The Grid Walk Test and the Modified Neurological Severity Score.

Grid Walk Test: The Grid Walk Test, also known as the

foot-fault test, is a widely used method to assess motor coordination and sensorimotor deficits in rodent models of stroke. In this test, rats were allowed to freely traverse a $45 \text{ cm} \times 45 \text{ cm}$ grid. As the animals moved, the number of foot placement errors (foot faults) was recorded. The score was calculated as the percentage of foot errors relative to the total number of footfalls, providing an objective measure of limb coordination and motor impairment. Healthy rats typically exhibit few foot faults, whereas ischemic rats display a marked increase in errors, reflecting deficits in motor control and coordination (33, 34).

Modified Neurological Severity Score: The mNSS is a comprehensive scoring system designed to evaluate neurological function in rodent stroke models, incorporating assessments of motor ability, sensory response, balance, and reflexes. The scale ranges from 0 to 18, where a score of 0 indicates normal neurological function and 18 represents severe impairment. Higher scores correspond to greater neurological deficits, enabling sensitive detection of functional changes following ischemic injury (35).

Histopathological examination

Brain tissues were fixed in 10% formalin for 24 hr to preserve morphological integrity and facilitate histopathological evaluation. Following fixation, samples underwent standard tissue processing, which included sequential dehydration in graded ethanol solutions, clearing with xylene, and embedding in paraffin wax. Sections of 5 μ m thickness were then prepared and stained using hematoxylin and eosin (H&E) for general histological assessment, as well as cresyl violet (Nissl staining) to evaluate neuronal integrity. Stained slides were examined under a light microscope (Olympus, Japan) to assess histopathological changes (36).

Oxidative stress assay

Oxidative stress parameters were assessed in brain tissue samples using established biochemical methods. Initially, protein concentration was determined by the Bradford assay with Coomassie Blue reagent (37). Levels of ROS were quantified using dichlorodihydrofluorescein diacetate (DCFH-DA) as a fluorescent probe, with measurements performed on a fluorometer (Jasco, Japan; model FP6200) at excitation and emission wavelengths of 480 nm and 520 nm, respectively. GSH content was measured in tissue homogenates using DTNB reagent, and absorbance was read at 405 nm with a microplate reader (37). Lipid peroxidation was evaluated by determining MDA levels, employing thiobarbituric acid as an indicator and measuring absorbance at 545 nm (38). PC content was assessed by treating samples with 2,4-dinitrophenylhydrazine (DNPH) and recording absorbance at 370 nm (39). Myeloperoxidase (MPO) activity was determined using a commercial kit (Nampox, Navand Salamat Co., Iran), based on the reaction of tetramethylbenzidine with hydrogen peroxide. The absorbance was measured at 650 nm (38). All assays were conducted according to the manufacturer's protocols or established literature methods, and results were normalized to protein concentration.

Inflammatory markers (NO and LDH)

Tissue nitric oxide levels were measured using the Natrix kit (Navand Salamat Co., Iran), which quantifies NO indirectly by detecting nitrite formed from the reaction with sulfanilic acid, resulting in an azo dye measured at 570 nm



using a microplate reader (39). This colorimetric approach is widely used in research for assessing NO and its metabolites in various biological samples, providing a reliable estimate of tissue NO content. Serum levels of lactate dehydrogenase were determined biochemically using the Pars Azmoon kit and analyzed with a Hitachi 902 autoanalyzer.

Gene expression

Gene expression analysis was performed to quantify the mRNA levels of TNF-a, IL-6, BAX, BCL2, NRF2, and HO-1 in rat brain tissue. Following euthanasia, brain samples were immediately placed in RNA shield solution (DENA Zist Asia, Iran) and stored at -80 °C to preserve RNA integrity. Total RNA was extracted using the Pars Toos Total RNA Extraction Kit (Pars Toos Company, Mashhad, Iran) based on the silica column method, ensuring high yield and purity as recommended for reliable downstream applications. The concentration and quality of RNA were assessed spectrophotometrically (Agilent Technologies, USA) at 230, 260, and 280 nm, and further confirmed by agarose gel electrophoresis with documentation (Biorad, USA). Complementary DNA (cDNA) was synthesized from the extracted RNA using the Pars Toos cDNA Synthesis Kit (Pars Toos Company, Iran) in a PCR thermocycler (Biorad, USA). Quantitative real-time PCR (qRT-PCR) was then conducted on a Corbett Rotorgene 6000 instrument (Qiagen, Germany) using gene-specific primers and a defined thermal cycling protocol. Glyceraldehyde 3-phosphate dehydrogenase (GAPDH) was used as the endogenous reference gene to normalize expression levels of the target genes, following established best practices for accurate normalization in qRT-PCR studies (39). Relative gene expression was calculated using the comparative 2-ΔΔCT method as detailed in the Table 2.

Quantification of drug levels in tissue samples

Brain tissue samples were homogenized in 2 ml of normal saline using a homogenizer operating at 10,000 RPM to ensure thorough extraction of the drug. The homogenate was centrifuged at 10,000 RPM for 20 min to separate cellular

debris, and the resulting supernatant was mixed with an equal volume of absolute ethanol to precipitate proteins. After vortexing for two minutes, the mixture was centrifuged again under the same conditions, and the clear supernatant was filtered through a syringe filter to remove any remaining particulates. The prepared samples were then analyzed by HPLC using a Knauer Smartline system (Germany) equipped with UV detection set at 268 nm. Separation was achieved on a reverse-phase C18 column (250 mm × 4.6 mm) using a modified mobile phase composed of 80:20 (v/v) 0.1% acetic acid and acetonitrile, delivered at a flow rate of 1 mL/ min over a total run time of 10 min. This method enabled precise quantification of the drug concentration in brain tissue by comparing sample peak areas to those of calibration standards, thereby determining the percentage of drug present in the homogenized brain samples.

Statistical analysis

All data were analyzed using one-way analysis of variance (ANOVA), followed by Tukey's *post hoc* test for multiple comparisons. Statistical analyses were performed with Prism software (version 9). Results are expressed as mean \pm standard error of the mean (SEM), and a *P*-value of less than 0.05 was considered statistically significant.

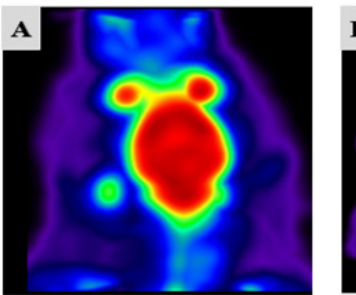
Results

Small-animal PET imaging

To evaluate brain status and validate our experimental procedures, we employed micro-positron emission tomography imaging to assess cerebral activity in both the sham (non-ischemic) and model (cerebral ischemia) groups. Micro-PET scans were performed one hour after intravenous administration of 18F-fluorodeoxyglucose (18F-FDG) by the tail vein. This technique enabled visualization of regional glucose metabolism in the brain. In the sham group, areas of high metabolic activity were indicated by red and yellow regions, reflecting robust glucose uptake. In contrast, the BCCAO model group exhibited green and blue regions, corresponding to reduced glucose utilization and hypometabolism following stroke induction.

Table 2. The sequence of primers and thermal conditions used for the analysis of gene expression in rats

| Genes | Primer | Thermal condition |
|-------|------------------------------|--|
| TNF-α | F: TCAGCCTCTTCTCATTCCTGCT | 95 °C, 5 min |
| | R: GCCATTGAACTGATGAGAGGGA | 40 cycles (95 °C, 20 sec; 63 °C, 20 s; 72 °C, 20 sec) 72 °, 5 min |
| IL-6 | F: TATACCACTTCACAAGTCGGAGG | 95 °C, 5 min |
| | R: GAATTGCCATTGCACAACTCTTT | 40 cycles (95 °C, 20 sec; 63 °C, 20 s; 72 °C, 20 sec) |
| Bcl-2 | F: CTGTGGATGACTGAGTACCTGA | 95 °C, 5 min |
| | R: AGCCAGGAGAAATCAAACAGAGG | 40 cycles (95 °C, 20 sec; 63 °C, 20 sec; 72 °C, 20 sec |
| | | 72°, 5 min |
| Bax | F: CCAAGAAGCTGAGCGAGTGT | 95 °C, 5 min |
| | R: TGTCCAGCCCATGATGGTTC | 40 cycles (95 °C, 20 sec ; 65 °C, 20 sec; 72 °C, 20 se |
| | | 72°, 5 min |
| NRF2 | F: ACATCCAGACAGACACCAGTGG | 95 °C, 5 min |
| но | R: GGAATGTCTCTGCCAAAAGCTG | 40 cycles (95 °C, 20 sec; 66 °C, 20 sec; 72 °C, 20 sec |
| | | 72°, 5 min |
| | F: CACAGCACTACGTAAAGCGTCT | 95 °C, 5 min |
| | R: GTAGCGGGTATATGCGTGGG | 40 cycles (95 °C, 20 sec; 63 °C, 20 sec; 72 °C, 20 se |
| | | 72°, 5 min |
| GAPDH | F: 5'CCCCCAATGTATCCGTTGTG 3' | 95 °C, 5 min |
| | R: 5'TAGCCCAGGATGCCCTTTAGT3' | 40 cycles (95 °C, 20 sec; 62 °C, 20 sec; 72 °C, 20 sec 72°, 5min |
| | | |



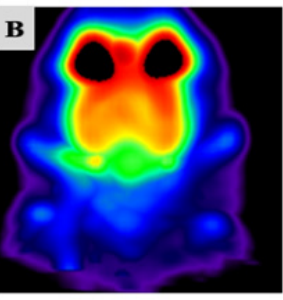


Figure 1. Representative micro-PET images depicting alterations in cerebral glucose metabolism in rat brains

(A) Sham group: rats that did not undergo bilateral common carotid artery occlusion surgery. (B) BCCAO group: rats subjected to the cerebral ischemia model via BCCAO, with imaging performed seven days post-procedure. BCCAO: Bilateral common carotid artery occlusion; PET: Positron Emission Tomography

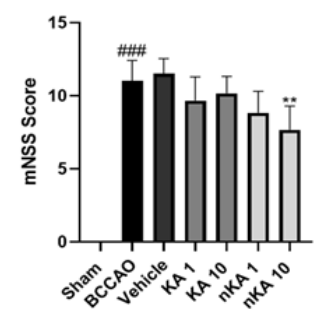
These findings demonstrate diminished glucose uptake and metabolic activity as characteristic consequences of cerebral ischemia and injury (Figure 1).

Behavioral tests

To evaluate changes in behavioral and neurological function, the Grid Walk and mNSS tests were conducted following the final drug treatment. After cerebral ischemia induction in the model group, both assessments revealed a significant increase in impairment and a reduction in normal motor and behavioral function compared to the sham group (### P<0.001 vs sham). The vehicle-treated group exhibited results comparable to the model group, with no significant differences observed. Administration of nKA at 10 mg/kg led to a significant improvement, as evidenced by a reduction in mNSS scores (** P<0.01 vs BCCAO group). NKA1 and nKA10 notably decrease error percentage in the Grid Walk test (** P<0.01 vs BCCAO group). Although the groups treated with KA at 1 and 10 mg/kg showed a trend toward improvement in both tests, these changes did not reach statistical significance compared to the model group (Figure 2).

Histopathological tests (Hematoxylin-Eosin and Nissl Staining)

Histopathological evaluation using hematoxylin-



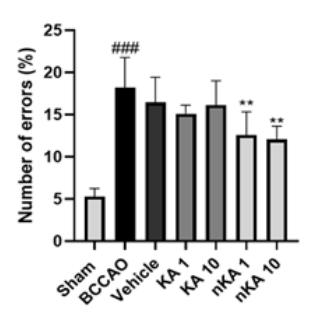


Figure 2. (A) Assessment of neurological function using the modified neurological severity score (mNSS) in rats

###P<0.001 compared to the sham group; **P<0.01 compared to the BCCAO group. (B) Evaluation of motor coordination by the grid-walking test. ###P<0.001 compared the sham group; **P<0.01 compared the BCCAO group

Statistical analysis was performed using one-way ANOVA followed by Tukey's post hoc test. Data are presented as mean \pm standard deviation (SD). BCCAO: Bilateral common carotid artery occlusion

eosin (H&E) and cresyl violet (Nissl) staining revealed distinct patterns of brain tissue injury and recovery across experimental groups following BCCAO and subsequent treatments. In coronal sections of the cortex, the sham group displayed well-preserved tissue architecture with clearly defined cell boundaries and nuclei, and neurons appeared morphologically intact, consistent with the absence of ischemic injury. In contrast, the BCCAO group exhibited pronounced histopathological alterations, including the presence of pigmented and shrunken neurons, indicative of acute ischemic damage.

Treatment with KA at both 1 and 10 mg/kg resulted in partial preservation of tissue structure compared to the untreated model group, as highlighted by regions with normal-appearing cells and areas containing degenerated or pigmented neurons (black arrow) in Figure 3. Notably, groups receiving nKA (1 and 10 mg/kg) demonstrated further improvement in tissue integrity, particularly in the hippocampus, where reduced neuronal degeneration and improved histological appearance were observed relative to the BCCAO group (Figure 4). Nissl staining further corroborated these findings: the sham group showed abundant neurons with intact morphology, while the BCCAO and vehicle groups exhibited marked neuronal loss,

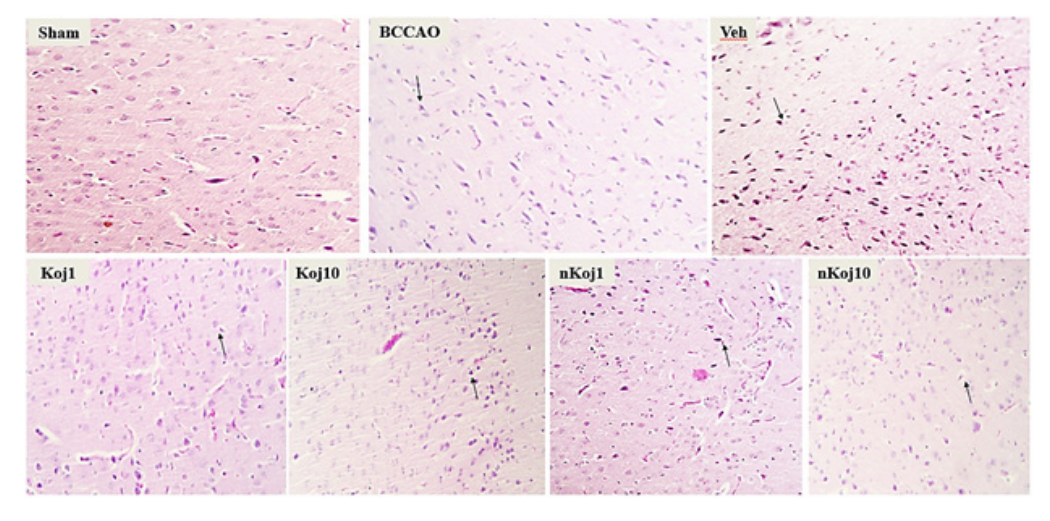


Figure 3. Representative hematoxylin and eosin (H&E) stained sections illustrating morphological alterations in rat brain tissue following BCCAO surgery The Sham group received normal saline without cerebral ischemia induction; the BCCAO group underwent bilateral common carotid artery occlusion; the Vehicle group received vehicle plus BCCAO; the KA1 and KA10 groups were treated with 1 mg/kg and 10 mg/kg kojic acid plus BCCAO, respectively; the nKA1 and nKA10 groups received 1 mg/kg and 10 mg/kg nano-kojic acid plus BCCAO, respectively. Black arrows indicate pyknotic cells characterized by condensed nuclei and cell shrinkage. Images were captured at 200× magnification, with a scale bar representing 100 μm. BCCAO: Bilateral common carotid artery occlusion

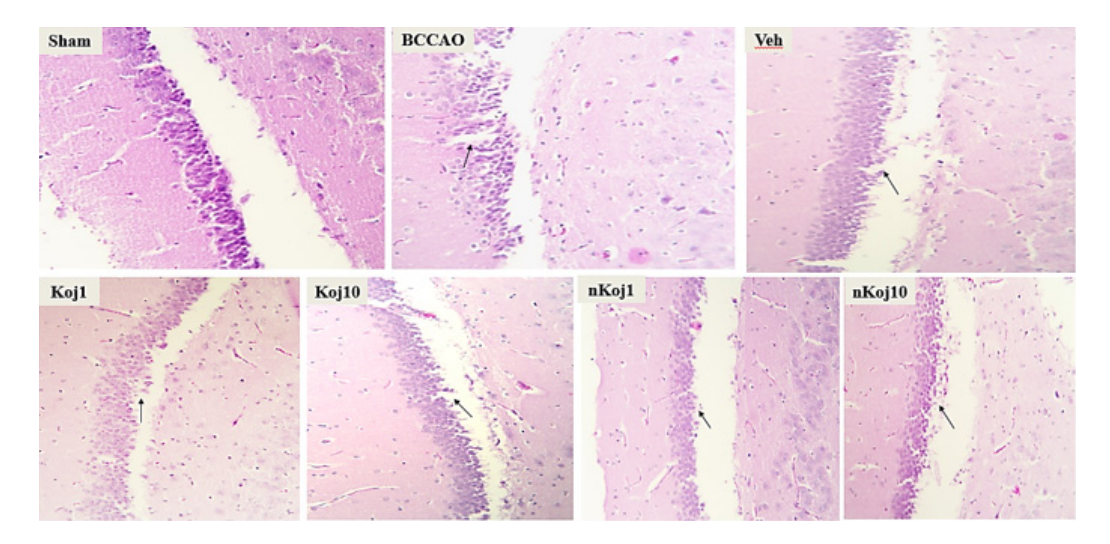


Figure 4. Representative hematoxylin and eosin (H&E) stained images showing morphological alterations in rat brain tissue across experimental groups The Sham group received normal saline without cerebral ischemia induction; the BCCAO group underwent bilateral common carotid artery occlusion; the Vehicle group was treated with vehicle plus BCCAO; the KA1 and KA10 groups received 1 mg/kg and 10 mg/kg kojic acid plus BCCAO, respectively; the nKA1 and nKA10 groups were administered 1 mg/kg and 10 mg/kg nano-kojic acid plus BCCAO, respectively. Black arrows indicate a lower number of cells compared to the sham group and the presence of pyknotic cells. All images were captured at 200× magnification, with a scale bar indicating 100 µm.

decreased nuclear density, and disrupted tissue architecture characterized by pyknotic nuclei, shrunken cytoplasm, and increased extracellular space. In contrast, the nKA 10 mg/kg group showed better preservation of neuronal structure and overall tissue integrity compared to the model group, as depicted in Figure 5.

Oxidative stress markers

Findings related to oxidative stress markers in brain tissue were assessed. In all tests, the BCCAO group was first compared with the sham group, indicated by the # symbol. This was followed by comparisons of the other five groups with the BCCAO group, denoted by the star symbol (*). Additionally, the KA and nKA groups were compared with the sham group, with a lack of significant difference indicated by the caret (^) symbol.

Assessment of oxidative stress markers in brain tissue

following BCCAO revealed significant alterations consistent with ischemic injury. ROS levels were markedly increased in the model group compared to the sham group. Treatment with KA (10 mg/kg) and nKA (10 mg/kg) significantly reduced ROS levels relative to the model group. GSH, a key non-enzymatic anti-oxidant, was depleted considerably in both the model and vehicle groups compared to the sham group. Administration of KA (1 mg/kg) and nKA (1 and 10 mg/kg) significantly increased GSH levels compared to the model group. MDA, a marker of lipid peroxidation and oxidative injury, was significantly elevated in the model group. Both the nKA (1 and 10 mg/kg) and KA (10 mg/kg) groups demonstrated significant reductions in MDA levels compared to the model group, indicating reduced lipid peroxidation.

PC content, an indicator of protein oxidation, was also significantly higher in the model group versus the sham group. Treatment with KA (1 and 10 mg/kg) and nKA

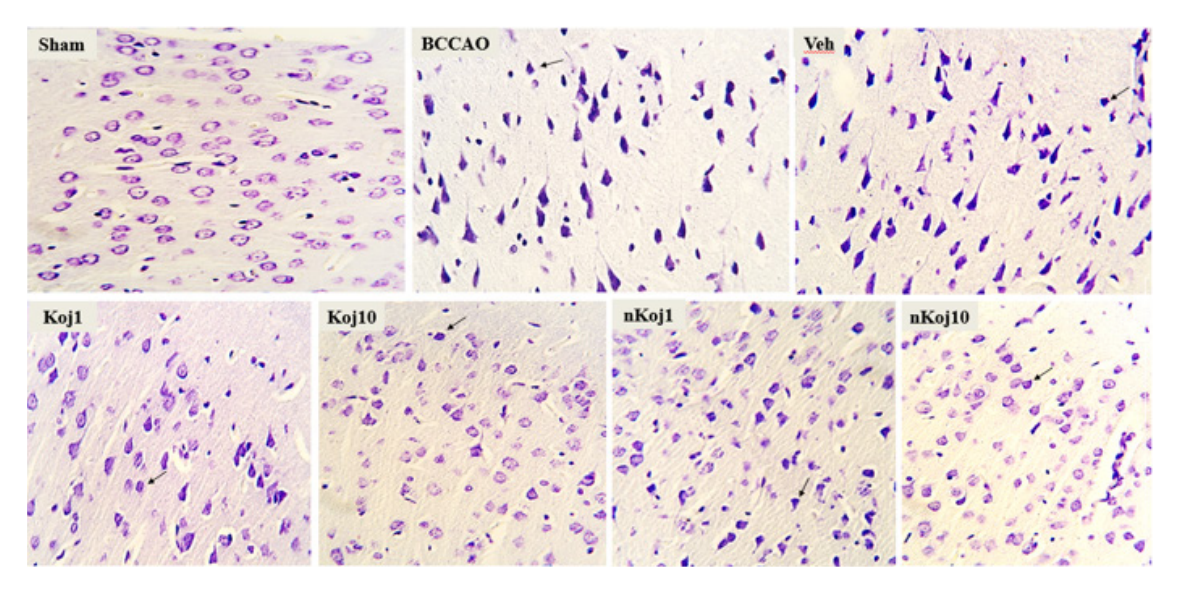


Figure 5. Representative cresyl violet (Nissl) stained sections illustrating morphological changes in rat brain tissue across experimental groups
The Sham group received normal saline without BCCAO induction; the BCCAO group underwent bilateral common carotid artery occlusion; the Vehicle group was administered vehicle plus BCCAO; the KA1 and KA10 groups received 1 mg/kg and 10 mg/kg kojic acid plus BCCAO, respectively; and the nKA1 and nKA10 groups were treated with 1 mg/kg and 10 mg/kg nano-kojic acid plus BCCAO, respectively. Black arrows indicate pyknotic cells characterized by condensed nuclei and cell shrinkage. All images were captured at 400× magnification, with a scale bar representing 100 μm.

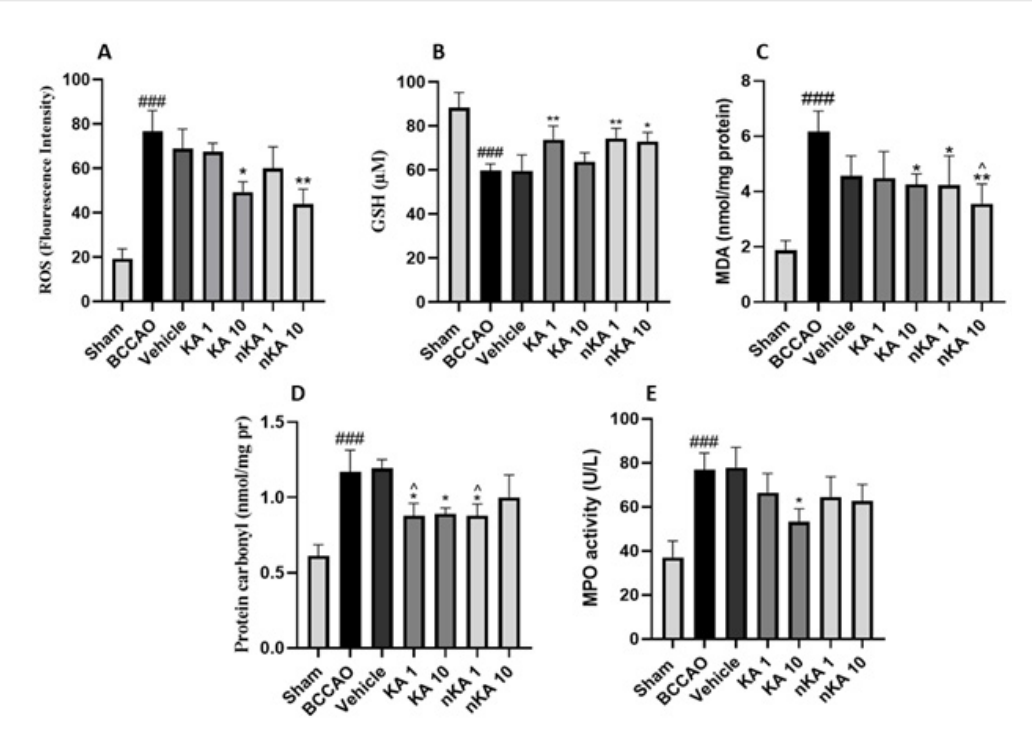


Figure 6. Alterations in oxidative stress and antioxidant biomarkers among rat experimental groups
(A) Reactive oxygen species (ROS), (B) glutathione (GSH), (C) malondialdehyde (MDA), (D) protein carbonyls (PC), and (E) myeloperoxidase (MPO) levels were quantified in all groups. The Sham group received normal saline without ischemia induction; the BCCAO group underwent bilateral common carotid artery occlusion without treatment; the Vehicle group was administered vehicle for 7 days post-BCCAO; the KA1 and KA10 groups were treated with 1 mg/kg and 10 mg/kg kojic acid intraperitoneally for 7 days after BCCAO, respectively; and the nKA1 and nKA10 groups received 1 mg/kg and 10 mg/kg nano-kojic acid intraperitoneally for seven days following BCCAO, respectively. Data are presented as mean ± standard deviation (SD) for each group.

###: P<0.001 significantly different from the sham group; *: P<0.05, significantly different from the BCCAO group; **: P<0.01 significantly different from the BCCAO group; ^: P<0.05, not significantly different from the sham group.

(1 mg/kg) resulted in significant decreases in PC levels compared to the model group. However, the KA (1 mg/kg) and nKA (1 mg/kg) groups showed no significant difference from the sham group.

Finally, MPO activity, which reflects neutrophil infiltration and oxidative inflammatory response, was significantly increased in the model groups compared to the sham group, consistent with established models of BCCAO-induced neuroinflammation and oxidative stress. Only the KA (10 mg/kg) group showed a significant reduction in MPO activity compared to the model group, while other treatment groups did not exhibit significant changes. Overall, these results demonstrate that BCCAO induces marked oxidative stress in the brain, as evidenced by increased ROS, MDA, PC, and MPO activity, and decreased GSH levels. Treatment with KA and nKA, particularly at higher doses, effectively mitigated these oxidative disturbances (Figure 6).

Inflammatory markers (NO and LDH)

Assessment of inflammatory markers revealed significant alterations following BCCAO-induced cerebral ischemia. Indirect measurement of NO levels in brain tissue demonstrated a marked elevation in both the model BCCAO groups compared to the sham group. Treatment with KA at 1 mg/kg and nKA at 10 mg/kg resulted in a significant reduction in NO levels relative to the model group (A). Similarly, LDH concentrations were significantly higher in the model group than in the sham group. At the same time, administration of KA 10 mg/kg and nKA 10 mg/kg significantly decreased LDH levels compared to the model group (B). These findings indicate that both KA and its nano-formulation, particularly at higher doses, can attenuate key inflammatory markers following cerebral

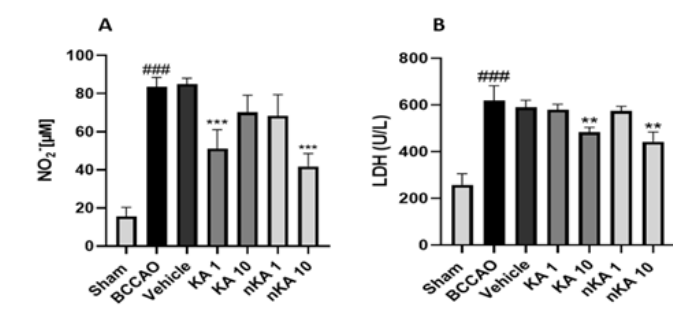


Figure 7. Serum levels of (A) nitric oxide (NO) and (B) lactate dehydrogenase (LDH) across all rat experimental groups

The Sham group received normal saline without brain ischemia induction; the BCCAO group underwent bilateral common carotid artery occlusion without treatment; the Vehicle group was administered vehicle following BCCAO; the KA1 and KA10 groups received 1 mg/kg and 10 mg/kg kojic acid intraperitoneally after BCCAO, respectively; and the nKA1 and nKA10 groups received 1 mg/kg and 10 mg/kg nano-kojic acid intraperitoneally for 7 days following BCCAO, respectively. Data are presented as mean ± standard deviation (SD) for each group.

Data are expressed as mean \pm standard deviation (SD) for each group.###: P<0.001 significantly different from the sham group, ***: P<0.01 compared with the BCCAO group, ***: P<0.001 compared with the BCCAO group

ischemia (Figure 7).

Gene expression

Gene expression profiling in rat brain tissue demonstrated significant alterations among the experimental groups (Figure 8). Compared to the sham group, the BCCAO model group showed a marked increase in pro-apoptotic (BAX) and pro-inflammatory (IL-6, TNF- α) genes, with a significant decrease in anti-apoptotic (BCL2) and anti-oxidant (NRF2, HO-1) genes (### P<0.001). Administration of nKA acid at both 1 and 10 mg/kg doses resulted in

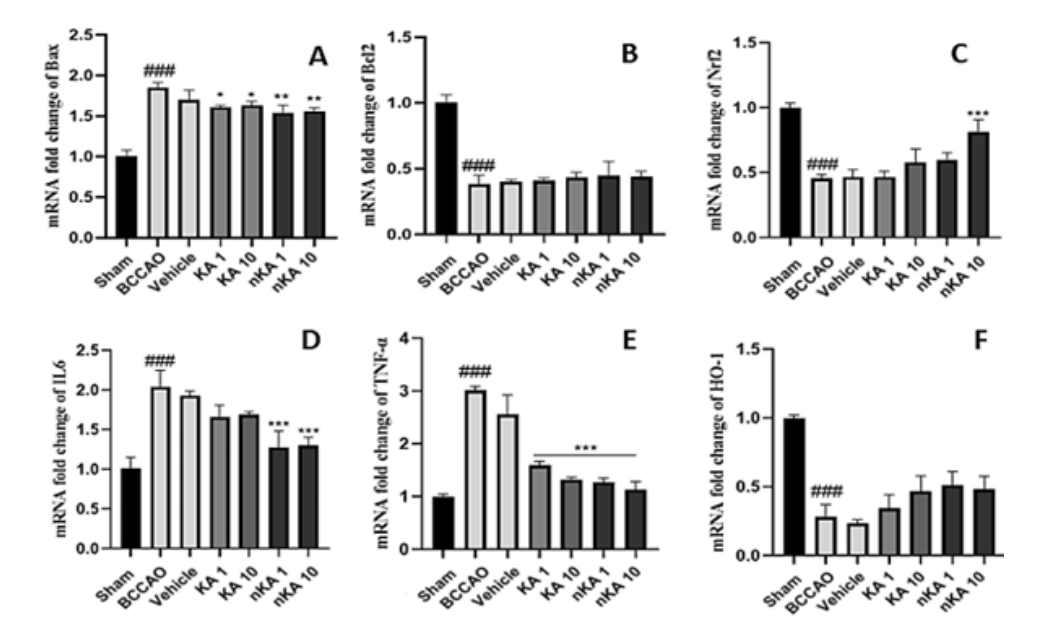


Figure 8. Relative mRNA expression levels of key apoptotic, anti-oxidant, and inflammatory markers in rat brain tissue (A) bax, (B) bcl2, (C) nrf2, (D) IL-6, (E) tnf-α, and (F) HO mRNA fold changes are shown for each experimental group. The Sham group received no cerebral ischemia induction; the BCCAO group underwent bilateral common carotid artery occlusion without treatment; the Vehicle group received vehicle following BCCAO surgery; the KA1 and KA10 groups were treated with 1 mg/kg and 10 mg/kg kojic acid intraperitoneally after BCCAO, respectively; the nKA1 and nKA10 groups received 1 mg/kg and 10 mg/kg nano-kojic acid intraperitoneally after BCCAO, respectively. Data are presented as mean ± standard deviation (SD) for each group.###: P<0.001 significantly different from the sham group; **, P<0.05 compared with the BCCAO group; **, P<0.01 compared with the BCCAO group.

significant reductions in IL-6 and TNF- α expression, while treatment with KA at 1 and 10 mg/kg also significantly decreased TNF- α levels (***P<0.001). Notably, an increase in NRF2 expression was observed only with the higher dose (10 mg/kg) of nKA (***P<0.001). In contrast, no significant differences were detected among the treatment groups for BCL2 and HO-1 gene expression. KA and nKA acid treatment did not significantly alter BCL2 or NRF2 expression. Additionally, the vehicle group did not exhibit significant changes compared to the BCCAO model group. These findings highlight the modulatory effects of KA and its nano-formulation on key apoptotic, inflammatory, and anti-oxidant gene pathways following cerebral ischemia.

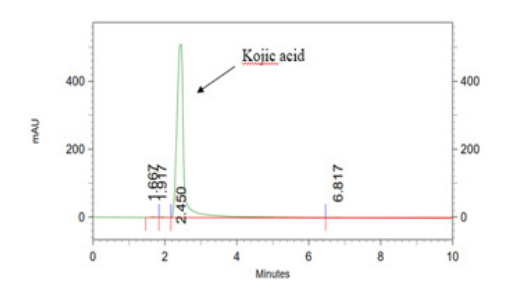
Quantification of drug levels in tissue samples

Quantitative analysis of KA in rat brain tissue was performed using HPLC, demonstrating the method's capability for specific and sensitive detection of both KA and its nano-formulation. Distinct chromatographic peaks for KA and nKA were observed at retention times of 2.45 and 2.75 minutes, respectively (Figure 9). No significant

interfering peaks were detected at these retention times, confirming the assay's specificity for the analytes under the established chromatographic conditions. Following administration, the percentage of KA detected in brain tissue was 12.59% at a dose of 1 mg/kg and 4.63% at 10 mg/kg, while nKA was present at 17.9% for 1 mg/kg and 6.27% for 10 mg/kg. Importantly, this reduction in percentage does not imply a lower absolute concentration of the drug in the brain. In fact, our data show that with increasing doses, the actual concentration of the drug in the brain tissue increased, though in a non-linear fashion.

Discussion

Brain ischemia remains a leading cause of mortality and long-term disability worldwide, primarily resulting from cerebral hypoperfusion or vascular occlusion. Despite advances in ischemic stroke care, therapeutic options remain limited and are often associated with adverse effects, underscoring the urgent need for innovative neuroprotective strategies to mitigate ischemic injury and promote functional recovery (40-42). The bilateral common carotid artery



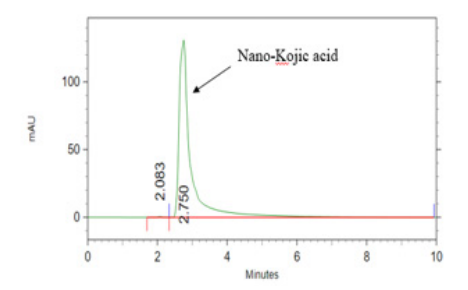


Figure 9. Representative high-performance rat liquid chromatography (HPLC) chromatograms of kojic acid (KA) and nano-kojic acid (nKA), monitored at 268 nm

Kojic acid eluted at a retention time of 2.45 min, while nKA exhibited a slightly delayed retention time of 2.75 min, reflecting formulation-dependent pharmacokinetic properties. The validated method demonstrated high analytical sensitivity, with a limit of detection (LOD) of 8.36 ng/mL and a limit of quantification (LOQ) of 27.89 ng/mL, ensuring precise quantification of both compounds in neural tissue matrices.



occlusion model serves as a well-characterized preclinical system for studying global cerebral ischemia, where both the ischemic event and subsequent reperfusion trigger distinct yet interconnected injury cascades. Central to this pathophysiology lies a pathological triad of oxidative stress, neuroinflammation, and apoptotic signaling mechanisms that drive neurodegeneration, manifest behaviorally as cognitive-motor deficits and potentially fatal outcomes (43-45). These pathological processes collectively contribute to neuronal loss, cognitive-motor deficits, and increased mortality, emphasizing the need to target multiple injury pathways to achieve neuroprotection.

(5-hydroxy-2-hydroxymethyl-4H-pyran-4-one), a fungal-derived organic compound, is best known for its skin-lightening effects through tyrosinase inhibition. It also exhibits additional pharmacological benefits, including antioxidant, antibacterial, anti-inflammatory, and leukocytemodulating activities. Despite these recognized properties, the detailed mechanisms behind its multifaceted biological actions are not yet fully elucidated (28, 46). It exhibits low acute toxicity in rodents, with an oral LD₅₀ in rats exceeding 1000 mg/kg body weight, supporting its safety at gram-perkilogram doses (47). Preclinical studies in rodent models have demonstrated its neuroprotective effects against neuroinflammation and oxidative stress. Doses around 50 mg/kg elicit anti-inflammatory responses without reported toxicity in short-term administration (48). To further inform our dose selection, we conducted pilot studies to gain insights into the effective dose range and potential toxicity, confirming minimal adverse effects at lower doses.

In the present study, BCCAO induced significant cerebral hypometabolism, elevated oxidative markers, and increased neuroinflammatory cytokine levels in rats, accompanied by behavioral impairments and histopathological evidence of brain injury. Treatment with both KA and its nanoformulation conferred neuroprotective effects. Notably, nKA at 10 mg/kg produced significant improvements in motor coordination and neurological function, whereas conventional KA showed trends toward behavioral recovery that did not reach statistical significance. Histopathological analysis revealed enhanced neuronal preservation with both treatments, especially at higher doses. Regarding oxidative stress biomarkers, both KA and nKA at 10 mg/kg reduced ROS, while increases in GSH were observed in the KA1, nKA1, and nKA10 groups, consistent with enhanced endogenous anti-oxidant capacity. MDA and protein carbonyl content were reduced in KA10, nKA1, and nKA10. Inflammatory biomarkers such as TNF-α and IL-6 were significantly decreased, particularly in nKA-treated animals. Treatment with nKA10 resulted in significant reductions in LDH and NO levels, all recognized markers of tissue damage and systemic inflammation. The KA10 group also exhibited reductions in LDH. Importantly, MPO activity was not affected by nKA treatment, probably indicating that the beneficial effects of nKA are independent of MPO-related mechanisms.

Molecular analysis revealed an increase in Nrf2 expression in the nKA10 group and a reduction in the pro-apoptotic protein BAX in all treatment groups, though anti-apoptotic BCL2 and HO-1 levels remained unchanged. HPLC confirmed brain penetration of both KA and nKA, corroborating their central bioavailability. Collectively, these data suggest that KA, as well as its nanoformulation, mitigated cerebral ischemic injury primarily through anti-

oxidant and anti-inflammatory mechanisms.

These findings support and extend research demonstrating the neuroprotective effects of KA in experimental models of oxidative stress and neuroinflammation. Oral administration of KA has been shown to reduce LPS-induced neuroinflammation by improving cognitive function and suppressing inflammatory mediators such as TNF-α and IL-1β. Moreover, KA treatment enhances Nrf2 gene expression. It decreases ROS levels, consistent with observed reductions in oxidative stress markers (ROS, MDA, PC) and inflammatory cytokines (TNF-α) in KA- and nKA-treated groups. However, in our study, the conventional form of KA did not induce a significant change in Nrf2 gene expression, which may be attributed to several factors, including variations in species (mice vs rats) and dosage regimens (49).

Furthermore, KA was shown to attenuate inflammation and restore impaired autophagy by suppressing NF- κ B and PI3K/AKT/mTOR signaling in an osteoarthritis model. This finding highlights a mechanism through which KA modulates cellular homeostasis under oxidative stress, a pathway potentially relevant to ischemic brain injury given the critical role of autophagy in neuronal survival (50). Our observed reductions in apoptotic marker BAX and oxidative damage support a similar anti-apoptotic effect in cerebral ischemia.

Khan et al. (2021) further corroborated KA's neuroprotective role in an amyloid-β (Aβ)-induced Alzheimer's disease mouse model. They demonstrated decreased oxidative stress, lipid peroxidation, and neuroinflammation through the inhibition of TLR4/NFкВ signaling and pro-inflammatory cytokines, alongside improved synaptic function and memory. These results parallel our findings, including brain bioavailability confirmed by HPLC, reinforcing the translational potential of KA and its nanoformulation for neurodegenerative conditions characterized by oxidative and inflammatory pathology (24). Beyond neurological diseases, KA exhibits broad-spectrum anti-inflammatory and antimicrobial activities. Montazeri et al. (2019) reported that KA reduced parasitic load and tissue damage in experimental toxoplasmosis by modulating host immune responses, suggesting that its immunomodulatory effects may be broadly applicable in diverse inflammatory contexts (23). Additionally, KA administration mitigated hematological and oxidative damage in radiation-exposed animals, further emphasizing its anti-oxidative versatility (25, 51). Studies in reproductive biology provide mechanistic insights into KA's anti-apoptotic properties. Hu et al. (2024) showed that KA inhibited apoptosis in porcine spermatozoa by enhancing mitochondrial anti-oxidant defenses, decreasing cleaved caspase-3 and caspase-9 (52). These findings correspond with our observations of reduced BAX expression and oxidative stress in KA/nKA-treated ischemic brains. Kotyzová et al. (2004) also reported that KA mitigated oxidative damage and regulated trace element homeostasis in iron-overloaded rodent models, a relevant mechanism given the role of iron-mediated oxidative injury in cerebral ischemia (53). Together, these studies reinforce the multimodal anti-oxidant and anti-apoptotic actions of KA that likely underlie its neuroprotective efficacy.

Advances in nanotechnology-based brain drug delivery support the superior efficacy of nKA in our study. A recent comprehensive review highlights NLCs as



second-generation lipid nanocarriers, offering improved biocompatibility and drug-loading capacity. They overcome the limitations of traditional delivery systems and provide targeted CNS delivery (54-56). This supports our findings that nKA surpasses conventional KA in behavioral assays, although their effects are relatively comparable in molecular tests. Nonetheless, we observed only a slight increase in brain penetration upon nano-formulation.

The biological activities of KA, including its antioxidant and anti-inflammatory effects, are attributable to its chemical structure. The hydroxyl groups on the pyrone ring facilitate hydrogen donation to neutralize free radicals, while metal chelation prevents Fenton reaction-mediated ROS generation (28). These mechanisms align with our findings, where KA and nKA reduced oxidative damage and inflammation in cerebral ischemia.

While our findings in general indicate a neuroprotective role for KA against cerebral ischemia, especially when formulated in NLC, a clear dose-response relationship was not observed in this study. This may be explained by receptor saturation, off-target effects, divergent endogenous inputs to the dependent variables of study, and non-linear kinetics (57-60). In particular, we did not find a 10-fold increase in brain concentration of KA when we increased the dose by 10 times in either of the conventional or NLC formulations. Our data show that with increasing doses, the actual concentration of the drug in the brain tissue increased, though in a non-linear fashion. For example, at 1 mg/kg of KA, the brain concentration was 0.311 μg/mg protein (12.59%). At 10 mg/kg, the concentration increased to 1.14 µg/mg protein, although the percentage decreased to 4.63%. Similarly, for nKA, the concentration increased from $0.443 \mu g/mg$ protein (17.9%) at 1 mg/kg to 1.550 $\mu g/mg$ protein (6.27%) at 10 mg/kg. These findings highlight a nonlinear dose-concentration relationship, which is common in CNS drug delivery and nanoparticle-based formulations.

Our study indicates that KA and its nKA significantly reduce oxidative stress markers, including MDA, and PC, as well as pro-apoptotic BAX and proinflammatory cytokines IL-6 and TNF-α, in a BCCAO model of cerebral ischemia in rats. These findings suggest that the neuroprotective effects of KA and nKA are likely mediated through attenuation of oxidative stress and neuroinflammation, with nKA potentially benefiting from enhanced brain penetration due to its formulation. However, the precise molecular pathways and their relative contributions remain incompletely understood, necessitating further studies to dissect the specific roles of these mechanisms through selective pathway inhibition. Comprehensive investigations are required to optimize dosing regimens and evaluate the long-term safety and efficacy of KA and nano-KA for potential clinical translation in stroke management.

Conclusion

This study demonstrates that nKA exhibits superior efficacy compared to conventional KA in improving neurobehavioral outcomes following the BCCAO model in rats. Meanwhile, the effects of KA in other tests are comparable to those of the nKA. The protective effects can be attributed to the intrinsic anti-oxidant and anti-inflammatory properties of KA, as well as a marginal increase in brain penetration upon nanoformulation. Our findings show significant attenuation of oxidative stress

markers and suppression of pro-inflammatory cytokines, supporting the therapeutic potential of the chemical as an adjunctive neuroprotective agent in cerebral ischemia management. Nevertheless, given the complexity of its underlying mechanisms, further in-depth studies are warranted to elucidate its precise mechanisms of action and assess chronic safety.

Acknowledgment

The authors gratefully acknowledge the support and facilities provided by Mazandaran University of Medical Sciences, Iran. The results presented in this article were part of a student thesis conducted at Mazandaran University of Medical Sciences.

Authors' Contributions

M S, F Sh, F T and M S designed the experiments; M Sh, M S, F T, and R N performed experiments and collected data; M Sh, M S, M S, and F Sh discussed the results and strategy; M S and F T supervised, directed, and managed the study; M S and F Sh approved the final version to be published.

Conflicts of Interest

The authors declare no competing interests.

Declaration

We acknowledge the use of Perplexity AI to enhance the language and readability of the manuscript. All data analyses and the preparation of figures and graphs were carried out independently, without the use of artificial intelligence.

Data Availability Statement

Data are available from the corresponding author upon reasonable request.

Ethical Approval

The ethical committee of the Mazandaran University of Medical Sciences (MAZUMS) approved this project (Reference Number: IR.MAZUMS.AEC.1403.018).

Funding

This study is supported by the Research Council of Mazandaran University of Medical Sciences, Sari, Iran [ID NO. 21563].

References

- 1. Wlodarek L, Alibhai FJ, Wu J, Li SH, Li RK. Stroke-induced neurological dysfunction in aged mice is attenuated by preconditioning with young sca-1+ stem cells. Stem Cells 2022; 40:564-576
- 2. Vaghari M, Moghaddam AH, Ranjbar M, Moradikor N. Protective effects of Japanese sake yeast on depressive-like behaviors, oxidative stress and inflammatory parameters in a rat model of global cerebral ischemia/reperfusion. Biochem Biophys Res Commun 2023; 674:97-101.
- 3. Azadi R, Mousavi SE, Kazemi NM, Yousefi-Manesh H, Rezayat SM, Jaafari MR. Anti-inflammatory efficacy of berberine nanomicelle for improvement of cerebral ischemia: Formulation, characterization and evaluation in bilateral common carotid artery occlusion rat model. BMC Pharmacol Toxicol 2021; 22:54-64.
- 4. Alemu C, Wudu H, Bogale B, Getachew Z, Nega A. Time to death and its determinant factors of stroke patients at gambella general hospital, gambella, ethiopia. Eur J Med Res 2024; 29:452-



462.

- 5. Goumtsa AF, Nguelefack-Mbuyo EP, Fofie CK, Fokoua AR, Becker A, Nguelefack TB. Neuroprotective effects of aframomum pruinosum seed extract against stroke in rat: Role of antioxidant and anti-inflammatory mechanisms. J Stroke Cerebrovasc Dis 2024; 33:107942.
- 6. Lei W, Zhuang H, Huang W, Sun J. Neuroinflammation and energy metabolism: A dual perspective on ischemic stroke. J Transl Med 2025; 23:413-424.
- 7. Salaudeen MA, Bello N, Danraka RN, Ammani ML. Understanding the pathophysiology of ischemic stroke: The basis of current therapies and opportunity for new ones. Biomolecules 2024; 14:305-327.
- 8. Akhtar W, Muazzam Khan M, Kumar S, Ahmad U, Husen A, Avirmed S. Pathophysiology of cerebral ischemia-reperfusion injury: An overview of oxidative stress and plant-based therapeutic approaches. Brain Res 2025; 1847:149308.
- 9. Dash UC, Bhol NK, Swain SK, Samal RR, Nayak PK, Raina V, *et al.* Oxidative stress and inflammation in the pathogenesis of neurological disorders: Mechanisms and implications. Acta Pharm Sin B 2025; 15:15-34.
- 10. Bai Y, Sui R, Zhang L, Bai B, Zhu Y, Jiang H. Resveratrol improves cognitive function in post-stroke depression rats by repressing inflammatory reactions and oxidative stress via the nrf2/ho-1 pathway. Neuroscience 2024; 541:50-63.
- 11. Jomova K, Alomar SY, Alwasel SH, Nepovimova E, Kuca K, Valko M. Several lines of antioxidant defense against oxidative stress: Antioxidant enzymes, nanomaterials with multiple enzymemimicking activities, and low-molecular-weight antioxidants. Arch Toxicol 2024; 98:1323-1367.
- 12. Alsbrook DL, Di Napoli M, Bhatia K, Biller J, Andalib S, Hinduja A, *et al.* Neuroinflammation in acute ischemic and hemorrhagic stroke. Curr Neurol Neurosci Rep 2023; 23:407-431.
- 13. Yang C, Hawkins KE, Dore S, Candelario-Jalil E. Neuroinflammatory mechanisms of blood-brain barrier damage in ischemic stroke. Am J Physiol Cell Physiol 2019; 316:C135-C153.
- 14. Jin XX, Fang MD, Hu LL, Yuan Y, Xu JF, Lu GG, *et al.* Elevated lactate dehydrogenase predicts poor prognosis of acute ischemic stroke. PLoS One 2022; 17:e0275651.
- 15. Singh R, Letai A, Sarosiek K. Regulation of apoptosis in health and disease: The balancing act of bcl-2 family proteins. Nat Rev Mol Cell Biol 2019; 20:175-193.
- 16. Snyder CM, Shroff EH, Liu J, Chandel NS. Nitric oxide induces cell death by regulating anti-apoptotic bcl-2 family members. PLoS One 2009: 4:e7059.
- 17. Abdel-Hameed SS, El-Daly M, Ahmed A-SF, Bekhit AA, Heeba GH. Dapoxetine prevents neuronal damage and improves functional outcomes in a model of ischemic stroke through the modulation of inflammation and oxidative stress. Naunyn Schmiedebergs Arch Pharmacol 2024; 397:253-266.
- 18. Birben E, Sahiner UM, Sackesen C, Erzurum S, Kalayci O. Oxidative stress and antioxidant defense. World Allergy Organ J 2012: 5:9-19
- 19. Wahul AB, Joshi PC, Kumar A, Chakravarty S. Transient global cerebral ischemia differentially affects cortex, striatum and hippocampus in bilateral common carotid arterial occlusion (bccao) mouse model. J Chem Neuroanat 2018; 92:1-15.
- 20. Wang H, Lu J, Gao WC, Ma X, Li N, Ding *Z, et al.* Donepezil down-regulates propionylation, 2-hydroxyisobutyrylation, butyrylation, succinylation, and crotonylation in the brain of bilateral common carotid artery occlusion-induced vascular dementia rats. Clin Exp Pharmacol Physiol 2020; 47:1731-1739.
- 21. Agarwal A, Vishnu VY, Sharma J, Bhatia R, Garg A, Dwivedi S, *et al.* Citicoline in acute ischemic stroke: A randomized controlled trial. PLoS One 2022; 17:e0269224.
- 22. Gonçalez ML, Marcussi DG, Calixto GMF, Corrêa MA, Chorilli M. Structural characterization and *in vitro* antioxidant activity of kojic dipalmitate loaded w/o/w multiple emulsions intended for skin disorders. BioMed research international 2015; 2015:304591.
- 23. Montazeri M, Emami S, Asgarian-Omran H, Azizi S, Sharif M,

- Sarvi S, *et al. In vitro* and *in vivo* evaluation of kojic acid against toxoplasma gondii in experimental models of acute toxoplasmosis. Exp Parasitol 2019; 200:7-12.
- 24. Khan A, Park TJ, Ikram M, Ahmad S, Ahmad R, Jo MG, *et al.* Antioxidative and anti-inflammatory effects of kojic acid in abeta-induced mouse model of alzheimer's disease. Mol Neurobiol 2021; 58:5127-5140.
- 25. Wang K, Li PF, Han CG, Du L, Liu C, Hu M, *et al.* Protective effects of kojic acid on the periphery blood and survival of beagle dogs after exposure to a lethal dose of gamma radiation. Radiat Res 2014; 182:666-673.
- 26. Khan BA, Waheed M, Hosny KM, Rizg WY, Murshid SS, Alharbi M, *et al.* Formulation and characterization of carbopol-934 based kojic acid-loaded smart nanocrystals: A solubility enhancement approach. Polymers (Basel) 2022; 14: 1489-1500.
- 27. Khezri K, Saeedi M, Morteza-Semnani K, Akbari J, Hedayatizadeh-Omran A. A promising and effective platform for delivering hydrophilic depigmenting agents in the treatment of cutaneous hyperpigmentation: Kojic acid nanostructured lipid carrier. Artif Cells Nanomed Biotechnol 2021; 49:38-47.
- 28. Zilles JC, Dos Santos FL, Kulkamp-Guerreiro IC, Contri RV. Biological activities and safety data of kojic acid and its derivatives: A review. Exp Dermatol 2022; 31:1500-1521.
- 29. Movassaghi S, Nadia Sharifi Z, Soleimani M, Joghataii MT, Hashemi M, Shafaroodi H, *et al.* Effect of pentoxifylline on ischemia- induced brain damage and spatial memory impairment in rat. Iran J Basic Med Sci 2012; 15:1083-1090.
- 30. Khezri K, Saeedi M, Morteza-Semnani K, Akbari J, Rostamkalaei SS. An emerging technology in lipid research for targeting hydrophilic drugs to the skin in the treatment of hyperpigmentation disorders: Kojic acid-solid lipid nanoparticles. Artif Cells Nanomed Biotechnol 2020; 48:841-853.
- 31. Tanha K, Seyedabadi M, Ghadiri H, Ay M. The effects of music and darkness on radionuclide distribution during mice fdg-pet scan. Iran J Vet Res 2025; 25:319-325.
- 32. Yousefi-Manesh H, Rashidian A, Hemmati S, Shirooie S, Sadeghi MA, Zarei N, *et al.* Therapeutic effects of modafinil in ischemic stroke; possible role of nf-kappab downregulation. Immunopharmacol Immunotoxicol 2019; 41:558-564.
- 33. Chang L, Yin CY, Wu HY, Tian BB, Zhu Y, Luo CX, *et al.* (+)-borneol is neuroprotective against permanent cerebral ischemia in rats by suppressing production of proinflammatory cytokines. J Biomed Res 2017; 31:306-314.
- 34. Ruan J, Yao Y. Behavioral tests in rodent models of stroke. Brain Hemorrhages 2020; 1:171-184.
- 35. Chen SF, Hsu CW, Huang WH, Wang JY. Post-injury baicalein improves histological and functional outcomes and reduces inflammatory cytokines after experimental traumatic brain injury. Br J Pharmacol 2008; 155:1279-1296.
- 36. Yang YY, Deng RR, Xiang DX. Naodesheng pills ameliorate cerebral ischemia reperfusion-induced ferroptosis via inhibition of the erk1/2 signaling pathway. Drug Des Devel Ther 2024; 18:1499-1514.
- 37. Naderi M, Seyedabadi M, Talebpour Amiri F, Akbari S, Shaki F. Rutin mitigates perfluorooctanoic acid-induced liver injury via modulation of oxidative stress, apoptosis, and inflammation. Iran J Basic Med Sci 2023; 26:1291-1297.
- 38. Rahimian R, Zirak MR, Seyedabadi M, Keshavarz M, Rashidian A, Kazmi S, *et al.* Protective effects of tropisetron on cerulein-induced acute pancreatitis in mice. Biomed Pharmacother 2017; 93:589-595.
- 39. Naderi M, Seyedabadi M, Amiri FT, Mohammadi E, Akbari S, Shaki F. Taurine protects against perfluorooctanoic acid-induced hepatotoxicity via inhibition of oxidative stress, inflammatory, and apoptotic pathways. Toxicol Res (Camb) 2023; 12:124-132.
- 40. Hezarkhani LA, Mansouri K, Salari N, Ammari-Allahyari M, Shahbazi H, MohamadYari M, *et al.* The relationship between blood omega-3 levels and the small vessel disease in ischemic stroke patients: A case-control study. Health Sci Rep 2025; 8:e70652.
- 41. Zhang W, Liu Y, Wu Y, Wang Z, Liu X, Hu Q, et al. Ros-



- triggered biomimetic hydrogel soft scaffold for ischemic stroke repair. Biomaterials 2025; 319:123217.
- 42. Liu X, Zhang Y, Ma Y, Han C, Tan S, Liu B, *et al.* Melatonin ameliorates ischemic brain injury in experimental stroke by regulation of mir-221 and ATG7 axis. Biochem Biophys Res Commun 2025; 760:151706.
- 43. Buch P, Sharma T, Airao V, Vaishnav D, Mani S, Rachamalla M, *et al.* Geraniol protects hippocampal cal neurons and improves functional outcomes in global model of stroke in rats. Chem Biol Drug Des 2023; 102:523-535.
- 44. Onimisi OB, Musa SA, Umana UE, Sambo SJ, Makena W. Tetrapleura tetraptera fruit phenolics fraction protects against the impact of ischemic stroke-induced hippocampal distortions and memory deficits in wistar rats. Anat Cell Biol 2024; 57:543-558.
- 45. Zhen G, Dore S. Optimized protocol to reduce variable outcomes for the bilateral common carotid artery occlusion model in mice. J Neurosci Methods 2007; 166:73-80.
- 46. Saeedi M, Eslamifar M, Khezri K. Kojic acid applications in cosmetic and pharmaceutical preparations. Biomed Pharmacother 2019; 110:582-593.
- 47. Burnett CL, Bergfeld WF, Belsito DV, Hill RA, Klaassen CD, Liebler DC, *et al.* Final report of the safety assessment of kojic acid as used in cosmetics. Int J Toxicol 2010; 29:244S-273.
- 48. Burdock GA, Soni MG, Carabin IG. Evaluation of health aspects of kojic acid in food. Regul Toxicol Pharmacol 2001; 33:80-101.
- 49. Áli W, Choe K, Park JS, Ahmad R, Park HY, Kang MH, *et al.* Kojic acid reverses lps-induced neuroinflammation and cognitive impairment by regulating the tlr4/nf-κb signaling pathway. Front Pharmacol 2024; 15:1443552.
- 50. Li J, Yu G, He Z, Huang H, Yang J, Nie M. Kojic acid alleviates osteoarthritis by attenuating inflammation and restoring impaired autophagy through regulating nf-kappab and pi3k/akt/mtor signaling pathways: An *in vivo* and *in vitro* study. Int Immunopharmacol 2025; 147:114022.
- 51. Hosseinimehr SJ, Emami S, Zakaryaee V, Ahmadi A, Moslemi

- D. Radioprotective effects of kojic acid against mortality induced by gamma irradiation in mice. Saudi Med J 2009; 30:490-493.
- 52. Hu B, Zhang H, Li Y, Xue Q, Yang M, Cao C, *et al.* Kojic acid inhibits pig sperm apoptosis and improves capacitated sperm state during liquid preservation at 17 degrees C. Mol Reprod Dev 2024; 91:e23738.
- 53. Kotyzová D, Eybl V, Koutensky J, Brtko J, Glattre E. Effects of kojic acid on oxidative damage and on iron and trace element level in iron-overloaded mice and rats. Cent Eur J Public Health 2004; 12 Suppl:S41-S44.
- 54. Khan S, Sharma A, Jain V. An overview of nanostructured lipid carriers and its application in drug delivery through different routes. Adv Pharm Bull 2022; 13:446-460.
- 55. Mall J, Naseem N, Haider MF, Rahman MA, Khan S, Siddiqui SN. Nanostructured lipid carriers as a drug delivery system: A comprehensive review with therapeutic applications. Intell Pharm 2025; 3:243-255.
- 56. Garg J, Pathania K, Sah SP, Pawar SV. Nanostructured lipid carriers: A promising drug carrier for targeting brain tumours. Future J Pharm Sci 2022; 8:25-55.
- 57. Lin W, Chen Y, Unadkat JD, Zhang X, Wu D, Heimbach T. Applications, challenges, and outlook for pbpk modeling and simulation: A regulatory, industrial and academic perspective. Pharm Res 2022; 39:1701-1731.
- 58. Conolly RB, Lutz WK. Nonmonotonic dose-response relationships: Mechanistic basis, kinetic modeling, and implications for risk assessment. Toxicol Sci 2004; 77:151-157.
- 59. Esmaeeli A, Ebrahimi F, Tanha K, Assadi M, Seyedabadi M. Low-dose angiotensin at(1) receptor beta-arrestin-biased ligand, trv027, protects against cisplatin-induced nephrotoxicity. Pharmacol Rep 2020; 72:1676-1684.
- 60. Esmaeeli Ä, Keshavarz Z, Dehdar F, Assadi M, Seyedabadi M. The effects of carvedilol, metoprolol and propranolol on cisplatin-induced kidney injury. Drug Chem Toxicol 2022; 45:1558-1564.